Deep sequencing analysis of CRISPR-escaping plasmid transconjugants in *Enterococcus faecalis*

Wenwen Huo[ab], Valerie J. Price[ab], Ardalan Sharifi[a], Michael Q. Zhang[a], and Kelli L. Palmer[a]*

Department of Biological Sciences, The University of Texas at Dallas, Richardson, Texas, USA[a]

[b]These authors contributed equally

*Corresponding author

E-mail: kelli.palmer@utdallas.edu (KLP)

Abstract

Enterococcus faecalis is a Gram-positive bacterium that natively colonizes the human gastrointestinal tract and opportunistically causes life-threatening infections. Multidrug-resistant (MDR) *E. faecalis* strains have emerged that are replete with mobile genetic elements (MGEs). Some *E. faecalis* strains possesses CRISPR-Cas systems, which reduce the conjugation frequency of pheromone-responsive plasmids. However, many transconjugants still arise, and we have demonstrated in previous studies that *E. faecalis* can transiently maintain both a functional CRISPR-Cas system and a CRISPR-Cas target. In this study, we used serial passage and deep sequencing to analyze CRISPR array dynamics over time in transconjugants which possess both a functional CRISPR-Cas system and a CRISPR-Cas target. In the presence of antibiotic selection for the plasmid, we found that plasmids ultimately escape CRISPR defense via the emergence of compromised CRISPR-Cas defense in host populations. As a consequence, these populations have enhanced abilities to acquire a second antibiotic resistance plasmid. In the absence of antibiotic selection, plasmids are lost from wild-type but not Δ*cas9* host populations over time. We conclude that the adaptive immune system of *E. faecalis* becomes compromised under antibiotic selection for MGEs, generating populations with enhanced abilities to undergo horizontal gene transfer.

Importance

Enterococcus faecalis is a leading cause of hospital-acquired infections and known disseminator of drug resistance among Gram-positive bacteria. One of the main means of antibiotic resistance dissemination among *E. faecalis* populations is mediated by plasmids. We have previously shown that strains with an active CRISPR-Cas system can reduce plasmid acquisition and thus limit the transmission of antibiotic resistance determinants. In this study, we observed subpopulations with transient co-existence of active CRISPR-Cas and a plasmid target. Through serial passage and targeted sequencing analysis on these populations, we

37 demonstrate that antibiotic treatment plays a key role in shaping the *E. faecalis* genome,
38 resulting in compromised genome defense that facilitates acquisition of other resistance
39 plasmids. These results are significant because they show how antibiotic selection for a plasmid
40 can alter the evolutionary trajectory of *E. faecalis* populations rendering them vulnerable to the
41 acceptance of multiple resistance plasmids.
42

Introduction

Enterococcus faecalis is a Gram-positive bacterium that normally colonizes the gastrointestinal tracts of humans and other animals (1). *E. faecalis* is also an opportunistic pathogen that can cause life-threatening antibiotic-resistant infections in hospitalized patients (2-4). Some *E. faecalis* strains have acquired antibiotic resistance through horizontal gene transfer (HGT), mediated primarily by plasmids and integrative conjugative elements (5-7). One of the most clinically relevant forms of HGT in *E. faecalis* is afforded through the pheromone-responsive plasmids (PRPs). The PRPs are narrow host range conjugative plasmids that disseminate antibiotic resistance and virulence genes among *E. faecalis* populations (5, 8-10). PRPs can also mobilize resistance genes to other clinically relevant bacterial pathogens (2, 11-14).

CRISPR-Cas systems provide prokaryotes with heritable sequence-specific genome defense against mobile genetic elements (MGEs) including plasmids and phage (15, 16). The structure and classification of these systems was reviewed recently (17). CRISPR-Cas systems consist of *cas* genes and a CRISPR array composed of spacers interspersed by direct and partially palindromic repeats (18, 19). Where sequence matches can be identified, the spacers generally have identity to MGEs of phage or plasmid origin (20). Some *E. faecalis* strains encode Type II CRISPR-Cas systems (21, 22) characterized by the Cas9 endonuclease, which cleaves DNA targets in a sequence-specific manner (23-25). Type II CRISPR-Cas defense is afforded in three stages. During adaptation, a Cas-protein complex, including Cas9, recognizes a protospacer from a newly encountered MGE in a PAM (Protospacer Adjacent Motif)-dependent manner, after which the protospacer is incorporated into the leader end of the CRISPR array (26-28). During expression, the CRISPR array is transcribed into pre-crRNA that is then then processed by the endonuclease RNase III in concert with Cas9 and tracrRNA (trans-activating crRNA), generating mature crRNAs (29). A mature crRNA bound by Cas9 and tracrRNA is an active targeting complex. When the bacterial host is invaded by a MGE that has

69 complementarity to a crRNA, the targeting complex recognizes the MGE in a PAM-dependent
70 manner and creates a double-stranded DNA break to prevent MGE invasion (30, 31).
71
72 We reported in a previous study that Type II CRISPR-Cas systems with spacers targeting PRPs
73 can reduce PRP dissemination in *E. faecalis* colony biofilms by ~80-fold (32). However, PRP
74 transconjugants were still observed at high densities (~10^5 cfu/mL) in these mating experiments.
75 In contrast, in several other bacterial species, no or few transconjugants were observed when
76 CRISPR-Cas defense in recipient cells targeted the conjugative element (16, 33-35). Some of
77 these studies sequenced the CRISPR-Cas loci of the CRISPR-escaping transconjugants,
78 determining that the transconjugants possessed mutations that compromised or inactivated
79 CRISPR-Cas defense (33, 34). Deletions of CRISPR spacers were commonly observed, as well
80 as mutations in *cas* genes (34, 36). These studies concluded that conjugation occurred into
81 recipient cells that had pre-existing mutations in CRISPR-Cas (33, 34). Similar observations
82 have been made for CRISPR-escape mutants obtained in plasmid transformation experiments
83 (37, 38). Collectively, these studies are consistent with the inability of cells to concomitantly
84 maintain both a functional CRISPR-Cas system and a target of the CRISPR-Cas system.
85 However, in recent studies from our lab using engineered shuttle plasmids mobilized by a PRP,
86 we determined that multidrug-resistant *E. faecalis* can transiently tolerate both CRISPR systems
87 and their plasmid targets, albeit at a fitness cost (reduced growth rate), and that selection can
88 determine the outcome of these conflicts (39). Specifically, CRISPR spacer deletion mutants
89 emerged over time when antibiotic selection for the plasmid was present, and plasmids were
90 lost when selection was absent (39). Similar observations of transient tolerance of
91 CRISPR/target co-maintenance have been made in *Pseudomonas aueruginosa* and *Listeria*
92 *monocytogenes* (40, 41).
93

In the present study, we further investigated how antibiotic selection impacts CRISPR-Cas systems and their targets in *E. faecalis,* specifically investigating PRP transconjugants using serial passage and deep sequencing experiments. Overall, our data provide evidence that antibiotic-selected PRP maintenance in *E. faecalis* can lead to compromised CRISPR-Cas defense and enhanced abilities to acquire other MGEs.

Results

Design of serial passage experiments. *E. faecalis* T11RF possesses a Type II CRISPR-Cas system, CRISPR3-Cas, that has 21 unique spacers (Fig S1) (32). Spacer 6 has 100% sequence identity to the *repB* gene of the model PRP pAD1 (42, 43), a well-characterized PRP that encodes a haemolytic bacteriocin, cytolysin; the virulence factor aggregation substance; and the toxin-antitoxin system *par* (8, 44). Previous research from our lab demonstrated that CRISPR3-Cas of T11RF significantly reduces the conjugation frequency of pAM714, a derivative of pAD1 conferring erythromycin resistance via *ermB* on Tn*917* (32). However, despite the activity of CRISPR3-Cas, a large number (~10^5) of presumptive T11RF(pAM714) transconjugants were obtained from these conjugation reactions. We set out to analyze these transconjugants further.

Conjugation reactions between *E. faecalis* OG1SSp(pAM714) donors and T11RF recipients were performed for 18 hours on agar plates without erythromycin selection as previously described (32). Biofilms were then scraped from the plates, resuspended and diluted, and plated on agar selective for donors, recipients, and transconjugants. Conjugation frequencies from these assays were previously reported (32). Colonies arising on transconjugant selection agar were used for this study (Fig 1a). We randomly selected transconjugant colonies from two mating schemes, T11RF(pAM714) and T11RFΔ*cas9*(pAM714); the Δ*cas9* strain possesses no CRISPR3-Cas activity through an in-frame deletion of the *cas9* coding region (32). We performed serial passage on a total of six T11RF(pAM714) transconjugants (referred to as

WT1-WT6) and six T11RFΔ*cas9*(pAM714) transconjugants (referred to as Δ1-Δ6) that were derived from two independent conjugation experiments. The transconjugant colonies were each resuspended in brain heart infusion (BHI) broth, and the percentage of erythromycin-resistant cells and the size and Sanger sequence of the CRISPR3 amplicon was determined for each (Fig S2; these data are discussed below). These data are referred to as "Day 0." Next, the colony resuspensions were split equally into BHI medium and BHI medium with erythromycin. These populations were then passaged daily over a period of 14 days. Every 24 h during the course of the passage, the percentage of erythromycin-resistant cells relative to the total viable population and the size and Sanger sequence of the CRISPR3 amplicon were determined.

At Day 0, erythromycin resistance was detected in both the T11RF(pAM714) and T11RFΔ*cas9*(pAM714) transconjugant populations, with the T11RF(pAM714) colonies having overall less erythromycin-resistant cells, indicative of active CRISPR defense (Fig S2a). The CRISPR3 arrays of all transconjugants analyzed were of wild-type size based on PCR (Fig S2b) and Sanger sequencing analysis.

Erythromycin resistance is eliminated by WT but not Δ*cas9* transconjugants during passage in non-selective medium. For serial passages in the absence of erythromycin, a gradual decrease in the frequency of erythromycin-resistant cells was observed for five of the six WT transconjugants (Fig 1b). In contrast, erythromycin resistance was stably maintained at high frequencies in all of the T11RFΔ*cas9*(pAM714) transconjugant populations (Fig 1b). CRISPR3 array size remained wild-type over the course of serial passage for both T11RF(pAM714) and T11RFΔ*cas9*(pAM714) transconjugant populations (Fig 1d and Fig S3).

The WT4 population did not exhibit erythromycin resistance loss in the absence of antibiotic selection. We Sanger-sequenced the *cas9* coding region of the WT4 population at Day 0 and

after 1 day of passage in the presence of erythromycin and identified a mutation resulting in an Ala749Thr substitution. Ala749 occurs within the RuvC nuclease domain in T11RF Cas9 and is conserved in the model *Streptococcus pyogenes* Cas9 (32). Due to the critical catalytic function of the RuvC domain, we hypothesize that the Ala749Thr substitution confers a loss of Cas9 function. We tested the ability of the BHI- and erythromycin-passaged WT4 populations to interfere with plasmid transfer using derivatives of the PRP, pCF10 (45), that are targeted by CRISPR3 spacers 1, 6, and 7. These experiments revealed that the Ala749 mutation indeed renders these populations deficient for CRISPR-Cas activity (Fig 2).

Under continuous antibiotic selection, CRISPR-Cas mutants emerge over time in WT transconjugant populations. When the transconjugant populations were serially passaged in the presence of erythromycin, we observed stable maintenance of erythromycin resistance in both WT and Δ*cas9* transconjugants (Fig 1c). We amplified the CRISPR3 region of erythromycin-passaged transconjugants and observed significant heterogeneity in the CRISPR3 array for WT transconjugant populations. By Day 14, four of the six T11RF(pAM714) transconjugant lineages had visibly reduced CRISPR3 arrays (Fig 1d). The variation in array size initiated sporadically over the 14 days and each transconjugant had a unique pattern (SFig 3). Sanger sequencing of the CRISPR3 array from Day 1 and Day 14 erythromycin-passaged populations revealed that S_6 was either deleted from the array or had low sequencing quality (Table 2). In contrast to WT populations, CRISPR3 arrays for the T11RFΔ*cas9*(pAM714) transconjugants were unchanged (Fig 1d and Table 2). We chose the Δ4 population as a representative of the T11RFΔ*cas9*(pAM714) transconjugant populations for future analyses.

To investigate the possibility of mutations within *cas* genes, we performed whole genome Illumina sequencing on five Day 14 erythromycin-passaged T11RF(pAM714) transconjugant populations and a control population, Δ4. We observed variation in the *cas9* sequence of the

WT1, WT2, and WT3 populations (Table 3). All of the mutations led to nonsynonymous changes and are predicted to result in a loss of function in Cas9 (Table 3). In addition to *cas9* mutations, some of the populations possessed variation in one or more genes, none of which are predicted to have an impact on the phenotypes observed in our study (STable2). No mutations were identified in the S_6 protospacer or PAM region of the *repB* gene in pAM714. However, we did identify a mutation within *repB*, not associated with the protospacer or PAM, in the WT2 population (STable2). The sequencing also allowed us to investigate the possibility of Tn*917* transposition into the T11RF chromosome. We observed no evidence of Tn*917* hopping into the T11 chromosome as all reads overlapping the ends of Tn*917* also overlapped the pAD1 reference sequence.

Reduced tolerance of S_6 in T11RF(pAM714) transconjugant populations. To attain greater resolution of CRISPR3 alleles present in our transconjugant populations, we used Illumina sequencing to sequence CRISPR3 amplicons from populations of interest. Using this method, we attained an average of 16 million reads for our amplicons (STable3). We first mapped CRISPR3 amplicon reads to the T11 reference sequence and calculated coverage depth to analyze mapping efficiency for BHI-passaged T11RF (lacking pAM714) (Fig. 3a) and the Δ4 transconjugant population passaged in erythromycin (Fig. 3b) as controls. We then expanded this analysis to the T11RF(pAM714) transconjugants. As expected, depletion of S_6 was detected in WT2, WT3, WT5, and WT6 populations after 14 days of passage with antibiotic selection (Fig 3d-g). For WT3, WT5, and WT6 populations, S_6 depletion was evident after one day of passage with selection (Fig 3e-g). For WT1, depletion of S_6 was not detected after 14 days passage with selection (Fig 3c), consistent with our Sanger sequencing results (Table 2).

To identify specific mutant CRISPR3 alleles in the amplicon sequencing, we manually constructed artificial CRISPR3 reference sequences for every possible spacer deletion event

198 (see Materials and Methods for more information). Each artificial reference is 96 bp in length
199 and contains two spacers connected by a T11 CRISPR3-Cas direct repeat: 5'-spacer[x]-repeat-
200 spacer[y]-3' (5'-SxRSy-3'), where spacer[x] and spacer[y] could be 30 bp upstream of the first
201 repeat (leader end; or S_0 hereafter; see Fig S1a), or any internal spacer within the CRISPR3
202 array (from spacer 1 to spacer 21; or S_1 to S_{21}; Fig S1a). The terminal repeat following S_{21} in the
203 CRISPR3 array is divergent from the direct repeat sequence, so references containing 5'-
204 spacer[x]-TerminalRepeat-S_T-3' (5'-S_xTRS_T-3') were constructed, where spacer[x] ranges from
205 S_0 to S_{21} and spacer S_T represents the sequence 30 bp downstream of the terminal repeat (Fig
206 S1a). In total, 484 references were constructed. Wild-type CRISPR3 alleles were represented
207 by the reference sequences where 5'-S_xR$S_{(x+1)}$-3' ($0 \leq x < 21$) and 5'-S_{21}TRS_T-3' and mutant
208 alleles were represented by 5'-S_xRS_y-3' ($y \neq x+1$). For the control population, which was BHI-
209 passaged T11RF lacking pAM714, all but 28 (Day 1) and 4 (Day 14) of the 484 possible alleles
210 were represented in our amplicon reads. We resolved the most abundant mutant CRISPR3
211 alleles in transconjugant populations by mapping amplicon reads to wild-type and mutant
212 CRISPR3 references (Fig 4). Of the five T11RF transconjugant populations analyzed, all other
213 than WT1 possessed at least one mutant CRISPR3 allele after 14 days of passage with
214 antibiotic selection, and each of those alleles lacked S_6 (Table 2).
215
216 We tested the ability of the Day 14 WT5 population to prevent the acquisition of pCF10 and
217 pCF10 derivatives that are targeted by CRISPR3 spacers 1, 6 and 7. Based on deep
218 sequencing data (Table 2), we expected that the WT5 population would interfere with transfer of
219 pCF10 bearing spacer 1, but not pCF10 bearing spacers 6 or 7. Compared to the BHI-passaged
220 WT5 population that significantly reduced the acquisition of each of the pCF10 derivatives, the
221 erythromycin-passaged WT5 population was unable to interfere with pCF10 bearing targets of
222 spacers 6 and 7 (Fig 2).
223

224 **Preference for spacer deletion over spacer inversion events.** Spacer deletion events due to
225 plasmid-CRISPR conflict have been previously reported (33, 37). However, the occurrence of
226 spacer inversions, where a leader distal spacer becomes more leader proximal, have not been
227 extensively studied. Due to the high sequence depth achieved in our study, we were able to
228 observe both events and monitor their dynamics for the duration of the serial passaging
229 experiments. Among our 484 artificial references, the spacer deletion group is represented by
230 the mutant alleles where a spacer has been removed from its natural position (5'-S_xRS_y-3'
231 where y > x+1 and 5'-S_xTRS_T-3' where x < 21), while the spacer inversion group is represented
232 by the mutant alleles where a terminal spacer has become more leader-proximal (5'-S_xRS_y-3'
233 where y < x). We calculated spacer deletion and spacer inversion rates for each spacer as
234 described in Materials and Methods.
235
236 In Day 1 and Day 14 BHI-passaged T11RF amplicons, we observed slightly higher spacer
237 deletion rates than spacer inversion rates for leader end spacers, suggesting that spacers at the
238 leader end are more readily deleted than inverted in naturally occurring CRISPR3 arrays (Fig
239 5a). On average, Day 14 T11RF showed slightly lower rates for deletion and inversion events
240 than Day 1 T11RF. However, the deletion and inversion rates were similar at spacers S_9-S_{15} for
241 Day 1 and Day 14 T11RF populations, indicating an equal chance of spacer deletion and
242 inversion (Fig 5a). Terminal end spacers are associated with decreased deletion and inversion
243 rates compared to leader end spacers. Interestingly, the inversion rates of terminal end spacers
244 are slightly higher than the rates for leader end spacers. We hypothesize that the increased
245 spacer inversion rates for terminal spacers is due to a greater number of homologous
246 sequences (direct repeats) toward the leader end of the array, suggesting that homologous
247 recombination played a role in spacer inversion events.
248

249 The deletion and inversion rates of five T11RF(pAM714) transconjugants and the Δ4 population
250 from Day 1 and Day 14 erythromycin passages were evaluated in the same manner as the
251 T11RF population. The distribution of deletion and inversion rates in the Δ4 and WT1
252 populations (Fig 5b and c) were similar to T11RF (Fig 5a). We did observe an elevated deletion
253 rate at S_5 for WT1 at Day 1, consistent with deep sequencing results which detected alleles
254 containing S_6 deletions in this population. The spacer deletion events in the other
255 T11RF(pAM714) erythromycin-passaged transconjugants (WT2, WT3, WT5 and WT6) have
256 unique positional preferences based on an increase in the average number of reads mapped to
257 the mutant allele references (Fig 5 d-g; red or black dots). Elevated spacer deletion rates were
258 frequently observed for spacers upstream of S_6, indicating a selective advantage for spacer
259 deletion events occurring upstream of S_6. Finally, we did not observe significant fluctuation of
260 spacer inversion rates in erythromycin-passaged transconjugants (Fig 5 d-g), indicating that
261 spacers are more readily deleted than rearranged.
262
263 **Spacer deletion is not exclusively RecA-dependent.** Under antibiotic selection,
264 T11RF(pAM714) transconjugants lost S_6 to resolve the conflict between CRISPR-Cas and its
265 target. The loss of S_6 was often coupled with the loss of surrounding spacers, ranging from S_1 to
266 S_{18} (Table 2). From our amplicon sequencing data, we noticed that the rearrangements
267 associated with shortened CRISPR3 arrays occurred between repeat-spacer junctions leaving
268 behind perfectly intact repeat-spacer-repeat sequences that are still functional for CRISPR
269 interference (Fig 2). This observation led us to hypothesize that either homologous
270 recombination or slippage during DNA replication plays a role in eliminating spacers from the
271 array, as has also been hypothesized by other groups (33, 34, 37, 38).
272
273 To study if homologous recombination had an impact on spacer loss, we constructed an in-
274 frame deletion of *recA* in T11RF, generating strain T11RFΔ*recA*, and used it as a recipient in

conjugation reactions with the donor OG1SSp(pAM714). We confirmed the presence of a wild type CRISPR3 array in the *recA* mutant with Sanger sequencing. Across three independent trials, only 12 transconjugant colonies were obtained. We selected two transconjugants (recA.TC1 and recA.TC2) for 14 day serial passaging with continuous erythromycin selection. PCR analysis for CRISPR3 amplicons of Day 0 recA.TC1 and recA.TC2 transconjugant colonies and the amplicons after 1 and 14 days of passage in erythromycin are shown in Figure 6. We used Sanger sequencing to assess spacer loss events in Day 1 and Day 14 populations, but not Day 0 transconjugants. We determined that recA.TC1 had lost S_6 after 1 day of passage in erythromycin, while the recA.TC2 population had a deletion of S_6-S_7. The same CRISPR3 alleles detected by Sanger sequencing after 1 day of passage were also observed at Day 14.

CRISPR-plasmid conflict leads to array-specific diversification in functionally linked CRISPR loci. Some *E. faecalis* strains possess the CRISPR1-Cas locus, a Type II CRISPR-Cas system that is distinct in sequence and function from the CRISPR3-Cas system of *E. faecalis* T11RF (22, 32). The CRISPR1-Cas system possesses identical repeats and is functionally linked to the orphan CRISPR2 locus, which occurs in all *E. faecalis* (22, 32, 39, 46). We wanted to determine if introducing a plasmid targeted by either CRISPR1-Cas or CRISPR2 would impact the integrity of the other locus within the same cell under continuous antibiotic selection for the plasmid target.

For these studies, we used the well-characterized human oral isolate OG1RF in combination with pKH12-derived plasmids (Table 1) that were described by Hullahalli et al (39). pKH12 is a chloramphenicol resistant shuttle vector that is mobilizable by the *oriT* sequence derived from the PRP, pCF10. Unlike pAD1, it does not encode any post segregational killing mechanisms and its antibiotic resistance determinant is not encoded on a transposable element. pKHS96 contains an engineered CRISPR1-Cas protospacer that is targeted by OG1RF CRISPR1-Cas

S_4 and pKHS5 contains an engineered CRISPR2 protospacer that is targeted by OG1RF CRISPR2 S_6. The consensus PAM sequence for both CRISPR1-Cas and CRISPR2 is NGG (32) and was included adjacent to the engineered protospacers. pKH12, pKHS96 and pKHS5 were each transformed into electrocompetent OG1RF. The initial integrity of the CRISPR1-Cas and CRISPR2 arrays, regardless of the plasmid transformed, was confirmed to be wild-type by Sanger sequencing.

Three transformants for each plasmid were selected to be used in serial passaging experiments. Each transformant was passaged in plain BHI medium and BHI medium supplemented with chloramphenicol for a period of 14 days. Similar to our observations for T11RF(pAM714) transconjugants, we observed plasmid loss in the absence of antibiotic (Fig 7a) and variation in the size of the CRISPR1 and CRISPR2 arrays after 14 days of passage in the presence of chloramphenicol (Fig 7b). Under antibiotic selection, all pKHS96 transformants had reduced CRISPR1 arrays (all with a loss of S_4), while the integrity of the CRISPR2 array remained intact. Similarly, after 14 days of antibiotic selection, two of three pKHS5 transformants had reduced CRISPR2 arrays, (both with a loss of S_6) while their CRISPR1 array remained of wild type size. These results show that CRISPR array mutations that relieve the conflict between CRISPR and its target are restricted to the locus that the crRNA is derived from. The otherwise functionally linked CRISPR array that coexists in the same cell experiences no diversification.

Discussion

It has been well documented that antibiotic use contributes to the dissemination of antibiotic resistance plasmids and the emergence of MDR organisms. However, bacteria encode genome defense systems such as CRISPR-Cas to reduce plasmid acquisition. The interactions of

CRISPR-Cas systems and naturally occurring resistance plasmids are poorly understood, which is of particular concern in the opportunistic pathogen *E. faecalis* due to its propensity to engage in intra- and interspecies HGT.

We previously demonstrated that the CRISPR3-Cas system of the natively drug sensitive *E. faecalis* isolate T11RF significantly reduced acquisition of the PRP pAM714 in a *cas9*- and spacer 6-dependent mechanism (32). The plasmid pAM714 is a derivative of the model PRP pAD1, obtained by spontaneous Tn*917* insertion between the *par* and *rep* loci of pAD1 (42, 47). Antibiotic resistance on PRPs is commonly encoded within conjugative and transposable elements that are integrated into the PRP backbone (5). In this regard, pAM714 is representative of the broader pool of PRPs conferring antibiotic resistance. Although not directly assessed for their contributions here, pAM714 also encodes cytolysin and aggregation substance, two well-studied virulence factors conferred by PRPs in *E. faecalis*.

In our previous study, we observed a substantial number of T11RF(pAM714) transconjugants, despite CRISPR3-Cas activity. Based on previous data in other organisms (33, 34, 38), we hypothesized that conjugation occurred into T11RF recipient cells with pre-existing CRISPR-inactivating mutations. However, recent data from our lab on another CRISPR-Cas system in *E. faecalis* and using different model strains indicated that this hypothesis was incomplete. Specifically, we observed spacer deletion mutants emerging over time in *E. faecalis* populations having CRISPR-Cas and a plasmid target in intracellular conflict (39). To attain deeper resolution, in the present study we tracked six distinct pAM714 transconjugant lineages that were predicted to experience intracellular conflict due to the presence of an active CRISPR-Cas system and its plasmid target. Our results describe multiple possible outcomes for conflict resolution between plasmids and CRISPR, with the outcome dependent on the presence or absence of antibiotic selection for the plasmid: 1) pre-existing *cas9* mutation (WT4); 2)

353 emergence of *cas9* mutation (WT1), mutant CRISPR arrays with internal spacer deletions (WT5
354 and WT6), or both (WT2 and WT3) during passage with selection; and 3) plasmid loss in the
355 absence of selection. Importantly, we did not observe spacer adaptation against the plasmid
356 during passage in the absence of selection; this in in contrast to other studies where spacer
357 acquisition against non-selected plasmids was observed (23). Rather, we hypothesize that
358 plasmid-containing cells are at a competitive disadvantage due to intracellular CRISPR/plasmid
359 conflict (39) and are depleted from the population over time, or, a slow-acting CRISPR-Cas
360 system progressively scrubs the plasmid from the population over time.
361
362 We used erythromycin resistance as a marker for pAM714 carriage. We acknowledge that the
363 erythromycin marker is encoded within Tn*917*, which could theoretically integrate into the
364 chromosome and escape CRISPR targeting of the pAM714 backbone. However, erythromycin
365 resistance was lost from five T11RF lineages passaged in the absence of selection, but not from
366 the Δ*cas9* transconjugants. This indicates that Tn*917* was lost, along with the pAM714
367 backbone, from the T11RF lineages in a CRISPR-dependent mechanism. Moreover, our
368 analysis of the whole genome sequencing from 8 independent populations found no evidence
369 for Tn*917* hopping under erythromycin selection.
370
371 The plasmid pAM714 encodes a toxin-antitoxin system (44, 48, 49). The system encodes a
372 stable toxin that will kill daughter cells that have not inherited a plasmid copy; an unstable
373 antitoxin is encoded from the same locus that blocks toxin translation in cells with proper
374 plasmid segregation. However, in our study, we observed a gradual decrease of erythromycin-
375 resistant cells when we passaged T11RF(pAM714) in BHI for 14 days, indicating that the toxin-
376 antitoxin system does not have robust activity in our experiments.
377

We performed high-coverage Illumina sequencing to assess the dynamics of the entire set of repeats and spacers that make up the CRISPR3 array. We determined that natural heterogeneity in CRISPR3 exists at a low frequency in wild-type T11RF populations. We reason that heterogeneity could result from slippage during DNA replication and/or recombination between CRISPR3 direct repeat sequences, consistent with previous research that proposed that heterogeneity exists within CRISPR arrays in bacterial populations (33, 34, 38). Furthermore, our results demonstrate that spacer deletion can occur in the absence of *recA*, which implicates DNA replication slippage in the emergence of mutant CRISPR alleles. However, the fact that we observed the occurrence of spacer inversions indicates that homologous recombination does play a role in the inherent allelic diversity of CRISPR arrays. It is likely that both recombination and replication slippage contribute to the emergence of heterogeneous CRISPR alleles. We do not have an estimate of which process has a greater effect, nor whether additional stresses beyond antibiotic selection could influence rates for each.

There were consequences to the resolution of CRISPR/plasmid conflicts in *E. faecalis* populations. In one case, in which pAM714 conjugated into a recipient with a pre-existing *cas9* mutation (WT4), the population could no longer impede entry of PRPs bearing CRISPR targets. For another population, WT5, its susceptibility to future plasmid transfer events was dependent upon whether it was passaged with erythromycin. The WT5 population passaged without erythromycin could impede entry of PRPs bearing CRISPR targets at levels comparable to the wild-type control. However, the WT5 population passaged with erythromycin, in which multiple CRISPR deletion alleles arose, lost the ability to defend against PRPs bearing certain spacer targets. In effect, antibiotic selection for pAM714 selected for the emergence of mutants with compromised CRISPR-Cas. We also observed that the acquisition frequencies of pCF10 and its derivatives were higher for all populations possessing pAM714 (WT5-Erm, WT4-BHI, and WT4-Erm). We infer that pAM714 enhances pCF10 conjugation frequency via an unknown mechanism. This was an unanticipated

404 additional outcome of the enforced maintenance of pAM714, and it remains to be determined
405 whether acquisition of other conjugative elements is also enhanced in pAM714-containing
406 populations.
407
408 In this study, we investigated outcomes of CRISPR/plasmid conflicts in *E. faecalis* using two
409 model strains (T11RF and OG1RF), three CRISPR loci (CRISPR3-Cas, and CRISPR1-Cas and
410 CRISPR2), two plasmid families (pAM714, a PRP, and the pKH12 family of mobilizable shuttle
411 vectors), and two antibiotic selection regimes (erythromycin and chloramphenicol). Our work
412 underscores the impact short-term antibiotic usage has on the evolutionary trajectory of the
413 opportunistic pathogen, *E. faecalis*.
414
415 **Materials and Methods**
416
417 **Strains, reagents, and routine molecular biology procedures.** Bacterial strains and plasmids
418 used in this study are listed in Table 1. *E. faecalis* strains were grown in Brain Heart Infusion
419 (BHI) broth or on agar plates at 37°C unless otherwise noted. Antibiotics were used for *E.*
420 *faecalis* at the following concentrations: erythromycin, 50 µg/mL; chloramphenicol, 15 µg/mL;
421 streptomycin, 500 µg/mL; spectinomycin, 500 µg/mL; rifampicin, 50 µg/mL; fusidic acid, 25
422 µg/mL. *Escherichia coli* strains used for plasmid propagation and were grown in lysogeny broth
423 (LB) broth or on agar plates at 37°C. Chloramphenicol was used at 15 µg/mL for *E. coli*. PCR
424 was performed using *Taq* (New England Biolabs) or Phusion (Fisher Scientific) polymerases.
425 Primer sequences used are in STable 1. Routine Sanger sequencing was carried out at the
426 Massachusetts General Hospital DNA core facility (Boston, MA). *E. faecalis* electrocompetent
427 cells were made using the lysozyme method as previously described (50).
428

Generation of mutant *E. faecalis* strains and plasmids. In-frame deletion of *recA* in T11RF was generated using a previously established protocol (51). Briefly, ~750 bp regions up- and downstream of *recA* in *E. faecalis* T11RF were amplified, digested, and ligated into pLT06 (51) to generate pWH*recA*. The resulting plasmid was transformed into competent T11RF cells via electroporation (50). Following transformation at 30°C, a shift to the non-permissive temperature of 42°C and counterselection on p-chloro-phenylalanine were performed to generate an in-frame, markerless deletion.

To insert the T11 CRISPR3 spacer 1 (S_1), S_6, and S_7 sequences and CRISPR3 PAM (TTGTA) into pCF10, 47 bp and 39 bp single stranded DNA oligos were annealed to each other to generate dsDNA with restriction enzyme overhangs for *BamHI* and *PstI*. The annealed oligos were ligated into the pLT06 derivative pWH107 that includes sequence from pCF10 *uvrB*, to insert these sequences into the *uvrB* gene of pCF10 by homologous recombination. A knock-in protocol was performed as previously described (32).

Conjugation experiments. *E. faecalis* donor and recipient strains were grown in BHI overnight to stationary phase. A 1:10 dilution was made for both donor and recipient cultures in fresh BHI broth and incubated for 1.5 hr to reach mid-exponential phase. A mixture of 100 µL donor cells and 900 µL recipient cells was pelleted and plated on BHI agar to allow conjugation. After 18 h incubation, the conjugation mixture was scraped from the plate using 2 mL 1X PBS supplemented with 2 mM EDTA. Serial dilutions were prepared from the conjugation mixture and plated on selective BHI agars. After 24-48 h incubation, colony forming units per milliliter (CFU/mL) was determined using plates with 30 - 300 colonies. The conjugation frequency was calculated as the CFU/mL of transconjugants divided by the CFU/mL of donors.

454 **Serial passage.** Transconjugant or transformant colonies were suspended in 50 µL BHI broth.
455 The 50 µL suspension was used as follows: 3 µL was used for PCR to confirm the integrity of
456 the CRISPR array, 10 µL was inoculated into plain BHI broth, another 10 µL was inoculated into
457 selective BHI broth for plasmid selection, and another 10 µL was used for serial dilution and
458 plating on selective medium to enumerate the initial number of plasmid-containing cells in the
459 transconjugant colonies. Broth cultures were incubated for 24 h, followed by 1:1000 dilution into
460 either fresh plain BHI or fresh selective BHI. At each 24 h interval, 3 µL of each culture from the
461 previous incubation was used for PCR to check CRISPR array integrity, and 10 µL was used for
462 serial dilution and plating on agars to determine CFU/mL for total viable cells and plasmid-
463 containing cells. The cultures were passaged in this manner for 14 days; cryopreserved culture
464 stocks were made daily in glycerol. To use the Day 14 transconjugant populations in
465 conjugation reactions, the glycerol stocks were completely thawed on ice, and 20 µL was
466 inoculated into plain BHI broth. The cultures were incubated for 6-8 h to allow them to reach
467 mid-exponential phase (OD_{600nm} ≈ 0.5–0.7), and 900 µL was used as recipient in conjugation
468 reactions as described above.
469
470 **Deep sequencing of CRISPR3 amplicons and genomic DNA.** For CRISPR3 amplicon
471 sequencing, 3 µL from a broth culture was used as template in PCR using Phusion Polymerase
472 with CR3_seq_F/R primers (STable1). The PCR products were purified using the Thermo
473 Scientific PCR purification kit (Thermo Scientific). Genomic DNA was isolated using the phenol-
474 chloroform method (52). The purified PCR amplicons and genomic DNA samples were
475 sequenced using 2 x 150 bp paired end sequencing chemistry by Molecular Research LP (MR
476 DNA; Texas).
477
478 **Whole genome sequencing analysis.** T11 supercontig and pAD1 plasmid contig references
479 were downloaded from NCBI (accession numbers: T11: NZ_GG688637.1-NZ_GG688649;

pAD1: AB007844, AF394225, AH011360, L01794, L19532, L37110, M84374, M87836, U00681, X17214, X62657, X62658). Reads were aligned to these references using default parameters in CLC Genomics Workbench (Qiagen) where ≥50% of each mapped read has ≥80% sequence identity to the reference. Variations occurring with ≥35% frequency at positions with ≥10X coverage between our samples and the reference contigs were detected using the Basic Variant Detector. At the same time, local realignment was performed, followed by Fixed Ploidy variant detection using default parameters and variants probability ≥90% in CLC Genomics Workbench. The basic variants and fixed ploidy variants were combined for each sequencing sample and subjected to manual inspection. The variants that were detected in the T11 genome from all samples were inferred to be variants in our parent T11 stock and were manually removed. The variants that were detected in pAD1 genome from all transconjugant samples were inferred to be variants in our pAM714 stock, hence were also manually removed. Next, variants within the CRISPR3 array were removed as we analyzed CRISPR3 alleles using a different approach (amplicon deep sequencing; see below). All variants detected from all populations were manually checked for coverage depth to eliminate the detection bias. The variants detected in all samples are shown in STable2.

Analysis of CRISPR3 amplicon sequencing. Reads from the 1,763 bp CRISPR3 amplicon were mapped to the T11 CRISPR3 reference (NZ_GG688647.1, positions 646834 - 648596) using stringent mapping conditions in CLC Genomics Workbench. The stringent mapping conditions require 100% of each mapped read to have ≥95% identity to the reference. The percent mapped reads were calculated by dividing the number of reads mapped by the total number of reads, these percentages are listed in STable3, step 1. The coverage depth was then calculated for each position within the PCR amplicon region using CLC Genomics Workbench, normalized using reads per million, and plotted against reference positions (Fig 3).

506 To further analyze CRISPR3 spacer deletions and rearrangements, we manually created
507 CRISPR3 references. The CRISPR3 amplicon references contain two spacers connected by a
508 T11 CRISPR3-Cas repeat: 5'-spacer[x]-repeat-spacer[y]-3' (5'-SxRSy-3'), where spacer[x] and
509 spacer[y] could be 30 bp upstream of the first repeat (leader end; or S_0 hereafter; Fig S1a), or
510 any internal spacer within the CRISPR3 array (from spacer 1 to spacer 21; or S_1 to S_{21}; Fig
511 S1a). Each manually generated CRISPR3 amplicon reference is 96 bp in length. The references
512 where y=x+1 represent wild-type alleles. The terminal repeat following S_{21} in the CRISPR3 array
513 is divergent from the regular direct repeat sequence, so references containing 5'-spacer[x]-
514 TerminalRepeat-S_T-3' (5'-S_xTRS$_T$-3') were constructed, where spacer[x] ranges from S_0 to S_{21}
515 and spacer S_T represents the sequence 30 bp downstream of the terminal repeat (Fig S1a). The
516 5'-S_{21}TRS$_T$-3' reference represents the wild-type. In total, 484 references with length of 96 bp
517 were generated for the CRISPR3 amplicon. Considering that the read length is 150 bp, we
518 manually split each read into two subsequences (one subsequence was 75 bp; with the
519 remainder of the read being the second subsequence) to enhance mapping efficiency, allowing
520 for retrieval of maximal sequence information. The split amplicon sequencing reads were
521 mapped to the 5'-SxRSy-3' and 5'-SxTRS$_T$-3' references using stringent mapping parameters in
522 CLC Genomics Workbench (Qiagen). The stringent mapping parameters require 100% of each
523 mapped read to be ≥95% identical to one unique reference. Thus, the sequencing reads from
524 different CRISPR alleles will be distinguished. These amplicon mapping results were applied to
525 the calculation of forward spacer deletion and backward spacer rearrangement rates.
526
527 To further evaluate the mapping efficiency, the unmapped reads from initial mapping to the T11
528 CRISPR3 reference (STable3, step 1) were subjected to additional quality control analysis. The
529 unmapped reads were mapped to the 484 manually created spacer[x]-repeat-spacer[y]
530 references using the same mapping parameters in CLC as above (STable3, step 2 mapping;
531 ignore unspecific mapping). The unmapped reads from step 2 were subjected to mapping to all

possible references (CRISPR3 region plus manually created references) using default mapping parameters, ignoring unspecific mapping (80% of each mapped read has at least 50% identity to the reference sequence; STable3, step 3 mapping). The unmapped reads from step 3 were mapped to all possible references using the default mapping parameters and randomly map unspecific matching reads (STable3, step 4 mapping).

Forward spacer deletion and backward spacer rearrangement. We observed two categories of mutant CRISPR3 alleles: 5'-S_xRS_y-3' (y > x+1) and 5'-S_xRS_y-3' (y < x). The forward deletion mutants with 5'-S_xRS_y-3' (y > x+1) are the result of spacer deletions, with spacers from S_{x+1} to S_{y-1} deleted; while the backward rearrangement mutants with 5'-S_xRS_y-3' (y < x) are the result of spacer rearrangement, where a downstream spacer S_y flips to become upstream of an upstream spacer S_x. To study if there were positional preferences, the average forward spacer deletion rate and backward spacer rearrangement rate was calculated for each 5'-S_x (0 < x < 21) within the CRISPR3 array. For each 5'-S_x, the average forward deletion and backward rearrangement rate are calculated as:

$$\mathrm{P}(\text{5'-Sx Forward}) = \frac{\#\ \text{mapped reads to the reference of 5'-SxRSy-3'}}{\sum_{y=x+1}^{n} \#\ \text{mapped reads to the references of 5'-SxRSy-3' and 5'-SnTRST-3'}}$$

$$\mathrm{P}(\text{5'-Sx Backward}) = \frac{\#\ \text{mapped reads to the reference of 5'-SxRSy-3'}}{\sum_{y=0}^{x-1} \#\ \text{mapped reads to the references of 5'-SxRSy-3'}}$$

where n is the total number of spacers within a CRISPR array, hence S_n represents terminal spacer, as described above (Fig S1a).

Accession number.

The sequencing data for amplicon and whole genome sequencing analysis of transconjugant populations has been deposited in the NCBI Sequence Read Archive under BioProject ID: PRJNA418345.

Acknowledgements

This work was supported by Public Health Service grant R01AI116610 to K.L.P and the Cecil H. and Ida Green Chair to M.Q.Z. We thank Karthik Hullahalli for construction of pKH12 and its derivatives. We thank Dr. Chen Jia for consultation on data analysis methods.

References

1. **Lebreton F, Willems RJL, Gilmore MS.** 2014. Enterococcus Diversity, Origins in Nature, and Gut Colonization. *In* Gilmore MS, Clewell DB, Ike Y, Shankar N (ed.), Enterococci: From Commensals to Leading Causes of Drug Resistant Infection, Boston.

2. **Kristich CJ, Djoric D, Little JL.** 2014. Genetic basis for vancomycin-enhanced cephalosporin susceptibility in vancomycin-resistant enterococci revealed using counterselection with dominant-negative thymidylate synthase. Antimicrobial agents and chemotherapy **58:**1556-1564.

3. **Uttley AH, George RC, Naidoo J, Woodford N, Johnson AP, Collins CH, Morrison D, Gilfillan AJ, Fitch LE, Heptonstall J.** 1989. High-level vancomycin-resistant enterococci causing hospital infections. Epidemiology and infection **103:**173-181.

4. **Huycke MM, Sahm DF, Gilmore MS.** 1998. Multiple-drug resistant enterococci: the nature of the problem and an agenda for the future. Emerging infectious diseases **4:**239.

5. **Clewell DB, Weaver KE, Dunny GM, Coque TM, Francia MV, Hayes F.** 2014. Extrachromosomal and Mobile Elements in Enterococci: Transmission, Maintenance, and Epidemiology. *In* Gilmore MS, Clewell DB, Ike Y, Shankar N (ed.), Enterococci: From Commensals to Leading Causes of Drug Resistant Infection, Boston.

6. **Palmer KL, Kos VN, Gilmore MS.** 2010. Horizontal gene transfer and the genomics of enterococcal antibiotic resistance. Current opinion in microbiology **13:**632-639.

7. **Hegstad K, Mikalsen T, Coque T, Werner G, Sundsfjord A.** 2010. Mobile genetic elements and their contribution to the emergence of antimicrobial resistant *Enterococcus faecalis* and *Enterococcus faecium*. Clinical microbiology and infection **16:**541-554.

584 8. **Clewell DB.** 2007. Properties of *Enterococcus faecalis* plasmid pAD1, a member of a
585 widely disseminated family of pheromone-responding, conjugative, virulence elements
586 encoding cytolysin. Plasmid **58:**205-227.

587 9. **Dunny GM.** 2007. The peptide pheromone-inducible conjugation system of
588 *Enterococcus faecalis* plasmid pCF10: cell-cell signalling, gene transfer, complexity and
589 evolution. Philosophical transactions of the Royal Society of London. Series B, Biological
590 sciences **362:**1185-1193.

591 10. **Gilmore MS, Segarra RA, Booth MC, Bogie CP, Hall LR, Clewell DB.** 1994. Genetic
592 structure of the *Enterococcus faecalis* plasmid pAD1-encoded cytolytic toxin system and
593 its relationship to lantibiotic determinants. Journal of bacteriology **176:**7335-7344.

594 11. **Jasni AS, Mullany P, Hussain H, Roberts AP.** 2010. Demonstration of conjugative
595 transposon (Tn*5397*)-mediated horizontal gene transfer between *Clostridium difficile* and
596 *Enterococcus faecalis*. Antimicrobial agents and chemotherapy **54:**4924-4926.

597 12. **Showsh SA, De Boever EH, Clewell DB.** 2001. Vancomycin Resistance Plasmid in
598 *Enterococcus faecalis* That Encodes Sensitivity to a Sex Pheromone Also Produced by
599 *Staphylococcus aureus*. Antimicrobial agents and chemotherapy **45:**2177-2178.

600 13. **Tsvetkova K, Marvaud JC, Lambert T.** 2010. Analysis of the mobilization functions of
601 the vancomycin resistance transposon Tn1549, a member of a new family of conjugative
602 elements. Journal of bacteriology **192:**702-713.

603 14. **Zhu W, Murray PR, Huskins WC, Jernigan JA, McDonald LC, Clark NC, Anderson**
604 **KF, McDougal LK, Hageman JC, Olsen-Rasmussen M, Frace M, Alangaden GJ,**
605 **Chenoweth C, Zervos MJ, Robinson-Dunn B, Schreckenberger PC, Reller LB,**
606 **Rudrik JT, Patel JB.** 2010. Dissemination of an *Enterococcus* Inc18-Like *vanA* plasmid
607 associated with vancomycin-resistant *Staphylococcus aureus*. Antimicrobial agents and
608 chemotherapy **54:**4314-4320.

609 15. **Barrangou R, Fremaux C, Deveau H, Richards M, Boyaval P, Moineau S, Romero**
610 **DA, Horvath P.** 2007. CRISPR provides acquired resistance against viruses in
611 prokaryotes. Science **315:**1709-1712.

612 16. **Marraffini LA, Sontheimer EJ.** 2008. CRISPR interference limits horizontal gene
613 transfer in staphylococci by targeting DNA. Science **322:**1843-1845.

614 17. **Makarova KS, Wolf YI, Alkhnbashi OS, Costa F, Shah SA, Saunders SJ, Barrangou**
615 **R, Brouns SJ, Charpentier E, Haft DH, Horvath P, Moineau S, Mojica FJ, Terns RM,**
616 **Terns MP, White MF, Yakunin AF, Garrett RA, van der Oost J, Backofen R, Koonin**

EV. 2015. An updated evolutionary classification of CRISPR-Cas systems. Nature reviews. Microbiology **13:**722-736.

18. **Jansen R, Embden JD, Gaastra W, Schouls LM.** 2002. Identification of genes that are associated with DNA repeats in prokaryotes. Mol Microbiol **43:**1565-1575.

19. **Mojica FJ, Diez-Villasenor C, Garcia-Martinez J, Soria E.** 2005. Intervening sequences of regularly spaced prokaryotic repeats derive from foreign genetic elements. Journal of molecular evolution **60:**174-182.

20. **Shmakov SA, Sitnik V, Makarova KS, Wolf YI, Severinov KV, Koonin EV.** 2017. The CRISPR Spacer Space Is Dominated by Sequences from Species-Specific Mobilomes. mBio **8:**e01397-01317.

21. **Bourgogne A, Garsin DA, Qin X, Singh KV, Sillanpaa J, Yerrapragada S, Ding Y, Dugan-Rocha S, Buhay C, Shen H, Chen G, Williams G, Muzny D, Maadani A, Fox KA, Gioia J, Chen L, Shang Y, Arias CA, Nallapareddy SR, Zhao M, Prakash VP, Chowdhury S, Jiang H, Gibbs RA, Murray BE, Highlander SK, Weinstock GM.** 2008. Large scale variation in *Enterococcus faecalis* illustrated by the genome analysis of strain OG1RF. Genome biology **9:**R110.

22. **Palmer KL, Gilmore MS.** 2010. Multidrug-resistant enterococci lack CRISPR-*cas*. MBio **1**.

23. **Garneau JE, Dupuis ME, Villion M, Romero DA, Barrangou R, Boyaval P, Fremaux C, Horvath P, Magadan AH, Moineau S.** 2010. The CRISPR/Cas bacterial immune system cleaves bacteriophage and plasmid DNA. Nature **468:**67-71.

24. **Jinek M, Chylinski K, Fonfara I, Hauer M, Doudna JA, Charpentier E.** 2012. A programmable dual-RNA-guided DNA endonuclease in adaptive bacterial immunity. Science **337:**816-821.

25. **Nishimasu H, Ran FA, Hsu PD, Konermann S, Shehata SI, Dohmae N, Ishitani R, Zhang F, Nureki O.** 2014. Crystal structure of Cas9 in complex with guide RNA and target DNA. Cell **156:**935-949.

26. **Anders C, Niewoehner O, Duerst A, Jinek M.** 2014. Structural basis of PAM-dependent target DNA recognition by the Cas9 endonuclease. Nature **513:**569-573.

27. **Wei Y, Terns RM, Terns MP.** 2015. Cas9 function and host genome sampling in Type II-A CRISPR-Cas adaptation. Genes Dev **29:**356-361.

28. **Heler R, Samai P, Modell JW, Weiner C, Goldberg GW, Bikard D, Marraffini LA.** 2015. Cas9 specifies functional viral targets during CRISPR–Cas adaptation. Nature **519:**199.

29. **Deltcheva E, Chylinski K, Sharma CM, Gonzales K, Chao Y, Pirzada ZA, Eckert MR, Vogel J, Charpentier E.** 2011. CRISPR RNA maturation by trans-encoded small RNA and host factor RNase III. Nature **471:**602-607.

30. **Sapranauskas R, Gasiunas G, Fremaux C, Barrangou R, Horvath P, Siksnys V.** 2011. The *Streptococcus thermophilus* CRISPR/Cas system provides immunity in *Escherichia coli*. Nucleic acids research **39:**9275-9282.

31. **Sternberg SH, Redding S, Jinek M, Greene EC, Doudna JA.** 2014. DNA interrogation by the CRISPR RNA-guided endonuclease Cas9. Nature **507:**62-67.

32. **Price VJ, Huo W, Sharifi A, Palmer KL.** 2016. CRISPR-Cas and Restriction-Modification Act Additively against Conjugative Antibiotic Resistance Plasmid Transfer in *Enterococcus faecalis*. mSphere **1:**e00064-00016.

33. **Jiang W, Maniv I, Arain F, Wang Y, Levin BR, Marraffini LA.** 2013. Dealing with the evolutionary downside of CRISPR immunity: bacteria and beneficial plasmids. PLoS genetics **9:**e1003844.

34. **Lopez-Sanchez MJ, Sauvage E, Da Cunha V, Clermont D, Ratsima Hariniaina E, Gonzalez-Zorn B, Poyart C, Rosinski-Chupin I, Glaser P.** 2012. The highly dynamic CRISPR1 system of *Streptococcus agalactiae* controls the diversity of its mobilome. Mol Microbiol **85:**1057-1071.

35. **Boudry P, Semenova E, Monot M, Datsenko KA, Lopatina A, Sekulovic O, Ospina-Bedoya M, Fortier L-C, Severinov K, Dupuy B.** 2015. Function of the CRISPR-Cas system of the human pathogen *Clostridium difficile*. MBio **6:**e01112-01115.

36. **Jiang W, Bikard D, Cox D, Zhang F, Marraffini LA.** 2013. RNA-guided editing of bacterial genomes using CRISPR-Cas systems. Nature biotechnology **31:**233-239.

37. **Bikard D, Hatoum-Aslan A, Mucida D, Marraffini LA.** 2012. CRISPR interference can prevent natural transformation and virulence acquisition during in vivo bacterial infection. Cell host & microbe **12:**177-186.

38. **Gudbergsdottir S, Deng L, Chen Z, Jensen JV, Jensen LR, She Q, Garrett RA.** 2011. Dynamic properties of the *Sulfolobus* CRISPR/Cas and CRISPR/Cmr systems

when challenged with vector-borne viral and plasmid genes and protospacers. Mol Microbiol **79:**35-49.

39. **Hullahalli K, Rodrigues M, Palmer KL.** 2017. Exploiting CRISPR-Cas to manipulate *Enterococcus faecalis* populations. Elife **6**.

40. **Hoyland-Kroghsbo NM, Paczkowski J, Mukherjee S, Broniewski J, Westra E, Bondy-Denomy J, Bassler BL.** 2017. Quorum sensing controls the *Pseudomonas aeruginosa* CRISPR-Cas adaptive immune system. Proceedings of the National Academy of Sciences of the United States of America **114:**131-135.

41. **Rauch BJ, Silvis MR, Hultquist JF, Waters CS, McGregor MJ, Krogan NJ, Bondy-Denomy J.** 2017. Inhibition of CRISPR-Cas9 with bacteriophage proteins. Cell **168:**150-158. e110.

42. **Clewell DB, Tomich PK, Gawron-Burke MC, Franke AE, Yagi Y, An FY.** 1982. Mapping of *Streptococcus faecalis* plasmids pAD1 and pAD2 and studies relating to transposition of Tn*917*. Journal of bacteriology **152:**1220-1230.

43. **Ike Y, Clewell DB, Segarra RA, Gilmore MS.** 1990. Genetic analysis of the pAD1 hemolysin/bacteriocin determinant in *Enterococcus faecalis*: Tn*917* insertional mutagenesis and cloning. Journal of bacteriology **172:**155-163.

44. **Weaver KE, Tritle DJ.** 1994. Identification and characterization of an *Enterococcus faecalis* plasmid pAD1-encoded stability determinant which produces two small RNA molecules necessary for its function. Plasmid **32:**168-181.

45. **Dunny G, Yuhasz M, Ehrenfeld E.** 1982. Genetic and physiological analysis of conjugation in *Streptococcus faecalis*. Journal of bacteriology **151:**855-859.

46. **Hullahalli K, Rodrigues M, Schmidt BD, Li X, Bhardwaj P, Palmer KL.** 2015. Comparative Analysis of the Orphan CRISPR2 Locus in 242 *Enterococcus faecalis* Strains. PloS one **10:**e0138890.

47. **Ike Y, Clewell DB.** 1984. Genetic analysis of the pAD1 pheromone response in *Streptococcus faecalis*, using transposon Tn*917* as an insertional mutagen. Journal of bacteriology **158:**777-783.

48. **Greenfield TJ, Ehli E, Kirshenmann T, Franch T, Gerdes K, Weaver KE.** 2000. The antisense RNA of the *par* locus of pAD1 regulates the expression of a 33-amino-acid toxic peptide by an unusual mechanism. Mol Microbiol **37:**652-660.

710 49. **Weaver KE, Clewell DB.** 1989. Construction of *Enterococcus faecalis* pAD1
711 miniplasmids: identification of a minimal pheromone response regulatory region and
712 evaluation of a novel pheromone-dependent growth inhibition. Plasmid **22:**106-119.

713 50. **Bae T, Kozlowicz B, Dunny GM.** 2002. Two targets in pCF10 DNA for PrgX binding:
714 their role in production of Qa and *prgX* mRNA and in regulation of pheromone-inducible
715 conjugation. Journal of molecular biology **315:**995-1007.

716 51. **Thurlow LR, Thomas VC, Hancock LE.** 2009. Capsular polysaccharide production in
717 *Enterococcus faecalis* and contribution of CpsF to capsule serospecificity. Journal of
718 bacteriology **191:**6203-6210.

719 52. **Manson JM, Keis S, Smith JMB, Cook GM.** 2003. A Clonal Lineage of VanA-Type
720 *Enterococcus faecalis* Predominates in Vancomycin-Resistant Enterococci Isolated in
721 New Zealand. Antimicrobial agents and chemotherapy **47:**204-210.

722 53. **Palmer KL, Godfrey P, Griggs A, Kos VN, Zucker J, Desjardins C, Cerqueira G,**
723 **Gevers D, Walker S, Wortman J, Feldgarden M, Haas B, Birren B, Gilmore MS.**
724 2012. Comparative genomics of enterococci: variation in *Enterococcus faecalis*, clade
725 structure in *E. faecium*, and defining characteristics of *E. gallinarum* and *E. casseliflavus*.
726 MBio **3:**e00318-00311.

727 54. **Gold OG, Jordan HV, van Houte J.** 1975. The prevalence of enterococci in the human
728 mouth and their pathogenicity in animal models. Archives of oral biology **20:**473-477.

729 55. **Perez-Casal J, Caparon MG, Scott JR.** 1991. Mry, a trans-acting positive regulator of
730 the M protein gene of *Streptococcus pyogenes* with similarity to the receptor proteins of
731 two-component regulatory systems. Journal of bacteriology **173:**2617-2624.

732 56. **Andersson AF, Banfield JF.** 2008. Virus population dynamics and acquired virus
733 resistance in natural microbial communities. Science **320:**1047-1050.
734

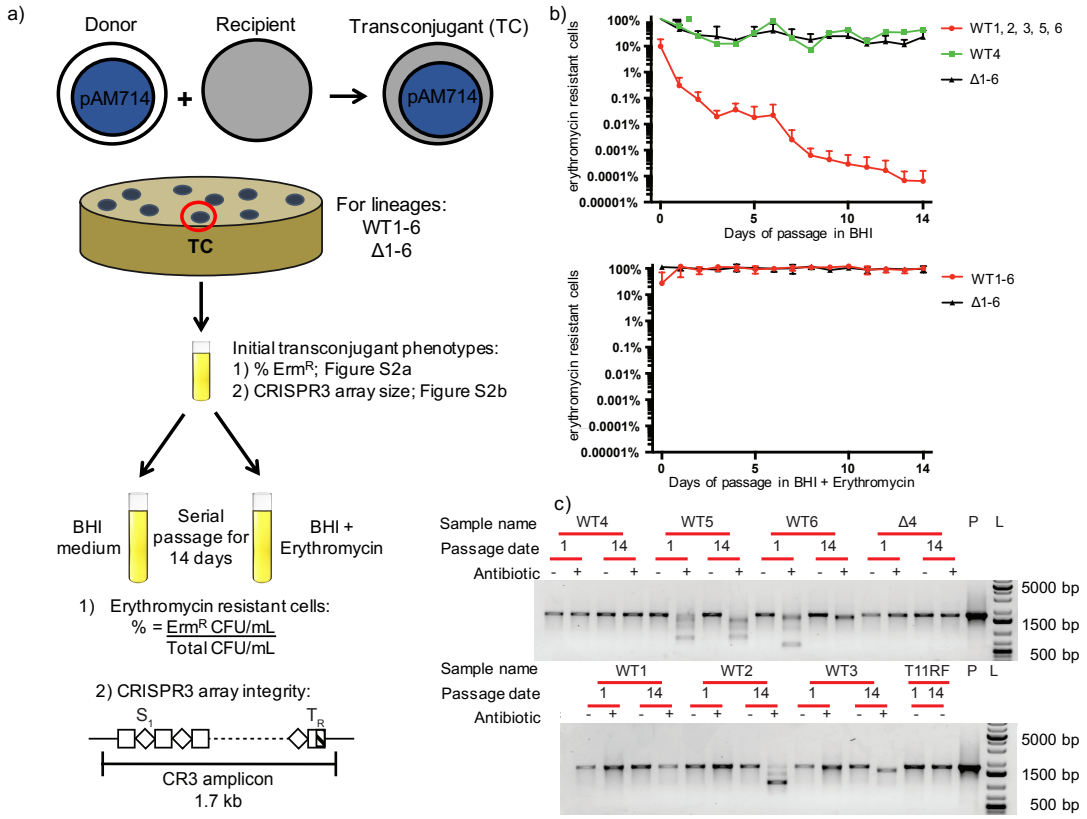

Figure 1. Antibiotic selection-specific phenotypes after serial passaging reflect outcomes of plasmid-host interactions. a) Design of serial passage experiment. Randomly selected T11RF(pAM714) and T11RFΔ*cas9*(pAM714) transconjugants were passaged for 14 days in the presence and absence of antibiotic selection for pAM714. These populations were monitored daily for: 1) erythromycin resistant cells by determining the percentage of erythromycin resistance relative to the total cell population and 2) deviations in the CRISPR3 array by amplifying the 1.7 kb region encompassing the CRISPR3 array. b) percentage of erythromycin resistance over the course of passage without (top) and with (bottom) antibiotic selection. WT populations are shown in green or red and Δ*cas9* populations are shown in black. c) CRISPR3 amplicon size from early (Day 1) and late (Day 14) passage dates for six WT transconjugant populations and a representative Δ*cas9* transconjugant population (Δ4). As a control, T11RF without pAM714 was passaged for 14 days and the CRISPR3 locus was queried (T11RF). P: positive control, T11RF genomic DNA. L: DNA ladder.

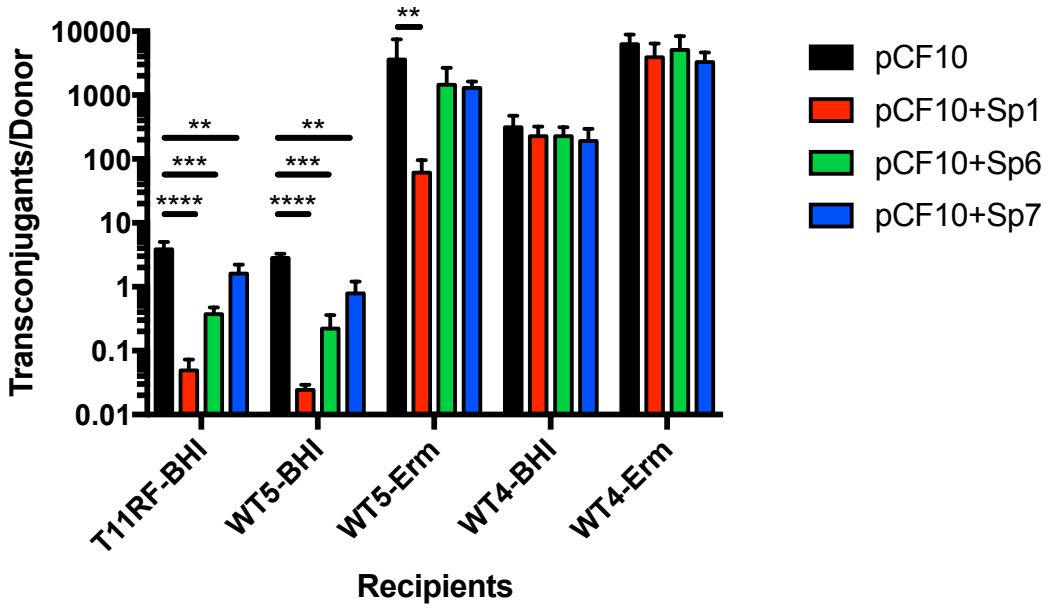

Figure 2. Compromised CRISPR-Cas primes populations for MGE acquisition. Day 14 transconjugant populations passaged in BHI and erythromycin were used as recipients in conjugation with OG1SSp pCF10 and derivatives with protospacers corresponding to spacers 1, 6 and 7 of the T11RF CRISPR3 array. The Day 14 BHI-passaged T11RF control population was used as recipient in conjugation, serving as control; pCF10 is not targeted by CRISPR3-Cas and pCF10+Sp1, Sp6 and Sp7 are all targeted. Based on the results of conjugation with the T11RF control population, we concluded that the degree of interference was different for each target where defense against a MGE bearing a target for S_7 was weak compared to S_1 and S_6. The graph shows the conjugation frequency or ratio of transconjugants to donors from mating reactions. Statistical significance was determined using a student's t-test; P-values: ** ≤ 0.01; *** ≤ 0.001; **** ≤ 0.0001.

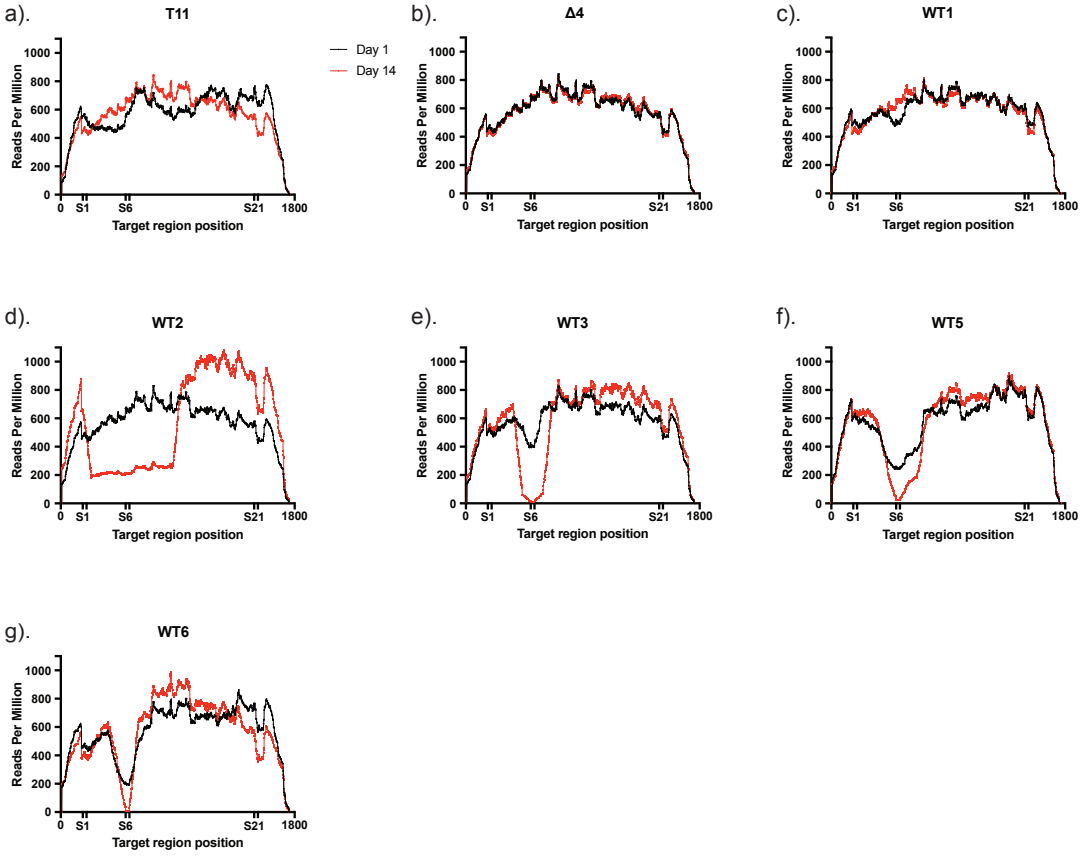

766
767
768 **Figure 3. Targeted sequencing revealed stochastic spacer loss after passage in**
769 **antibiotic.** The coverage depth is calculated for each position within the amplicon and
770 normalized using reads per million, which is then plotted against the genomic position. For each
771 sample, the results for Day 1 and Day 14 are represented in black and red lines, respectively.
772 The beginning and end of the regions along the amplicon corresponding to S_1, S_6 and S_{21} within
773 the CRISPR3 array are labeled with vertical hash marks on the x-axis. a) BHI passaged T11RF
774 parent strain. b) Erythromycin passaged Δ4 transconjugant. c-g) Erythromycin passaged WT
775 transconjugants. Here, the WT4 population is not included due to the inactivating *cas9* mutation,
776 as discussed in the main text.
777

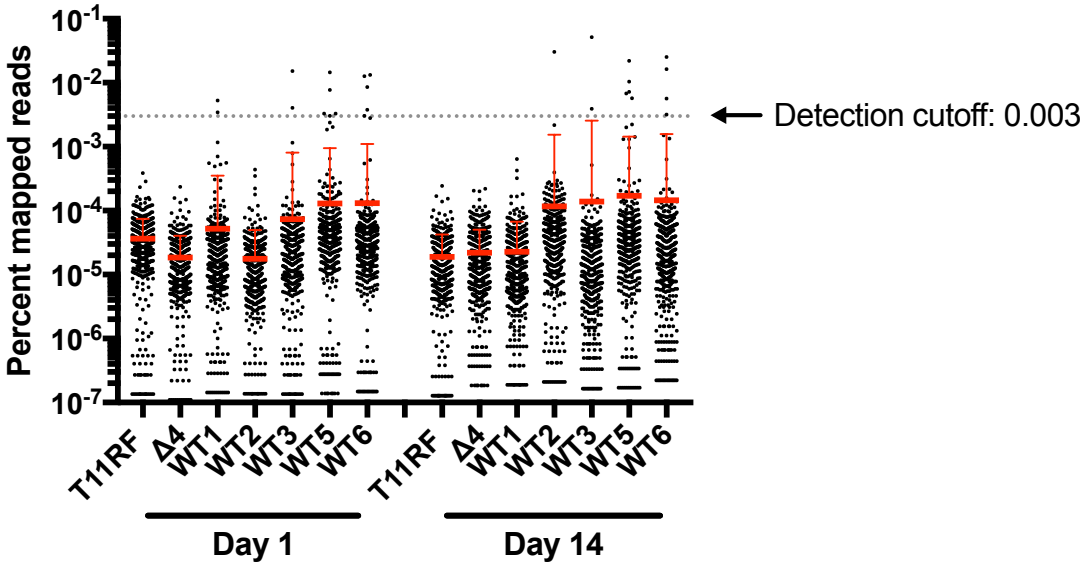

Figure 4. Distribution of mutant CRISPR3 array alleles among antibiotic-passaged wild-type transconjugants. Percent mapped reads were calculated for each artificial reference by dividing mapped reads at each position to the total number of mapped reads. The percent mapped reads to mutant alleles (dots) are shown here with average (thick red bar) and standard deviation (thin red bar). A detection cutoff value was applied so that mutant alleles with high abundances can be detected.

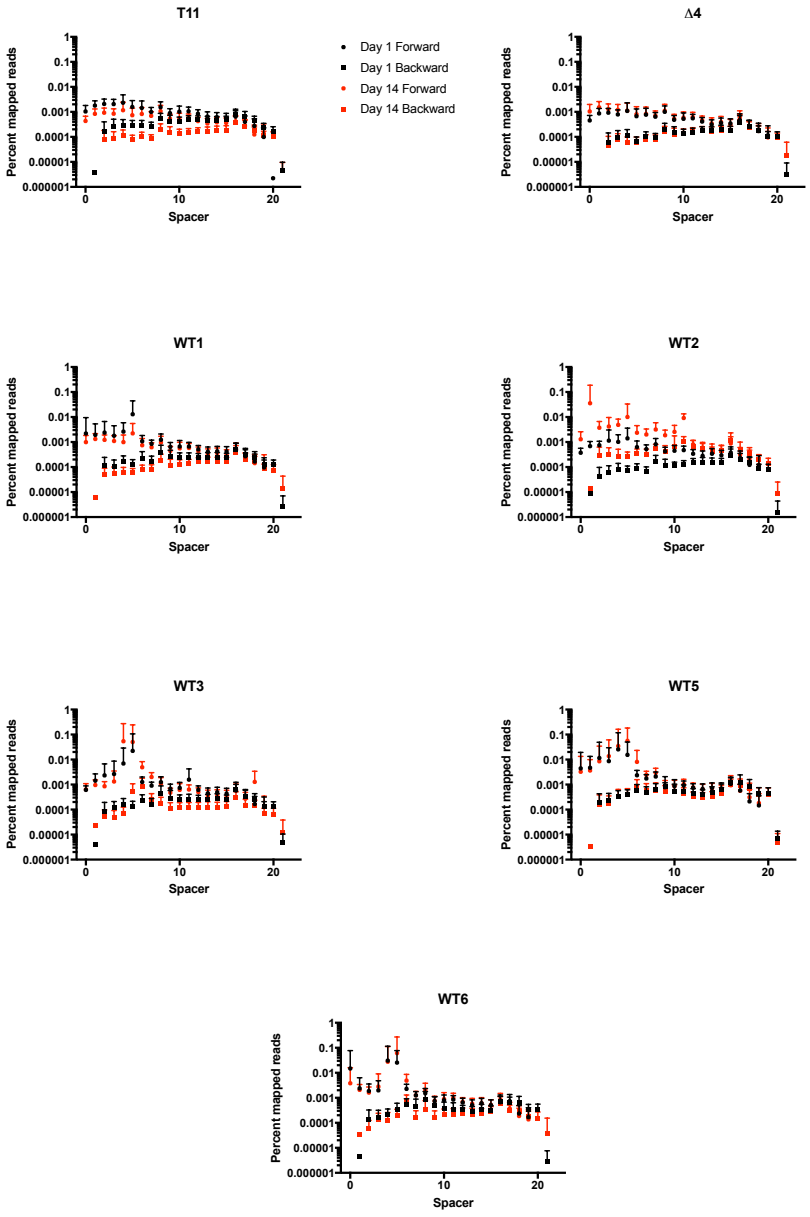

Figure 5. Mutant CRISPR alleles arise predominately through forward spacer deletion events. The forward spacer deletion and backward rearrangement rates (y-axis) were calculated for the CRISPR3 amplicon of each passaged population and are plotted against each spacer occurring in the CRISPR3 array shown on the x-axis. For each sample, the forward deletion (dots) and backward rearrangement (squares) rates for Day 1 and Day 14 of the passage are shown in black and red, respectively. a) BHI passaged T11RF parent strain. b) Erythromycin passaged Δ4 transconjugant. c-g) Erythromycin passaged WT transconjugants.

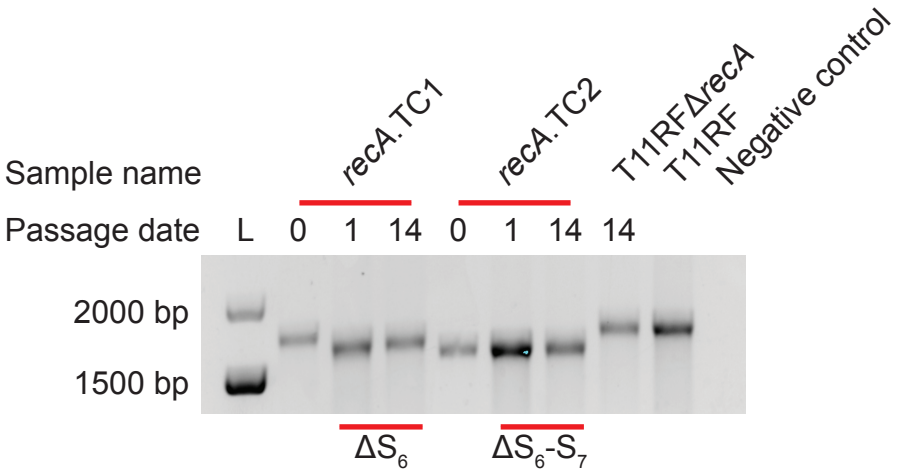

Figure 6. CRISPR3 array reduction is not dependent on RecA. Two randomly selected transconjugants were passaged *in vitro* with erythromycin selection and the CRISPR3 amplicon sizes were monitored using PCR and gel electrophoresis. As a control, the T11RFΔ*recA* parent strain was passaged in BHI and used as a control in PCR analysis. L: DNA Ladder.

a).

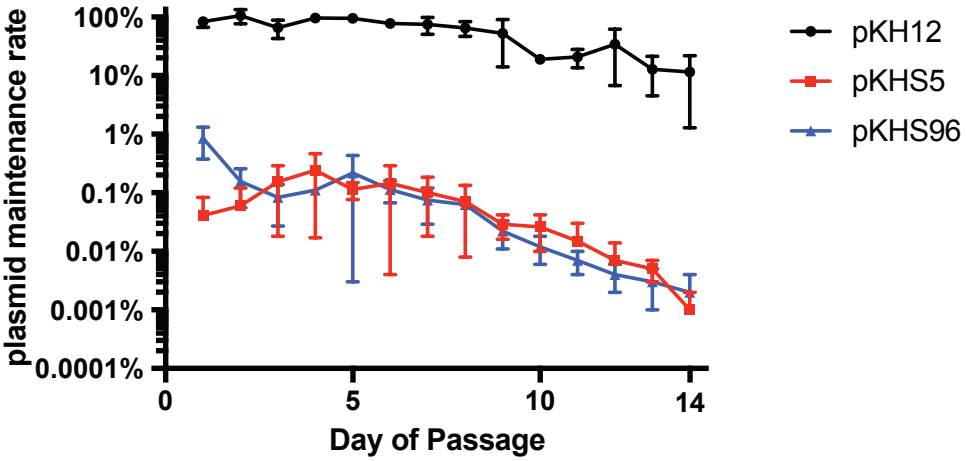

b).

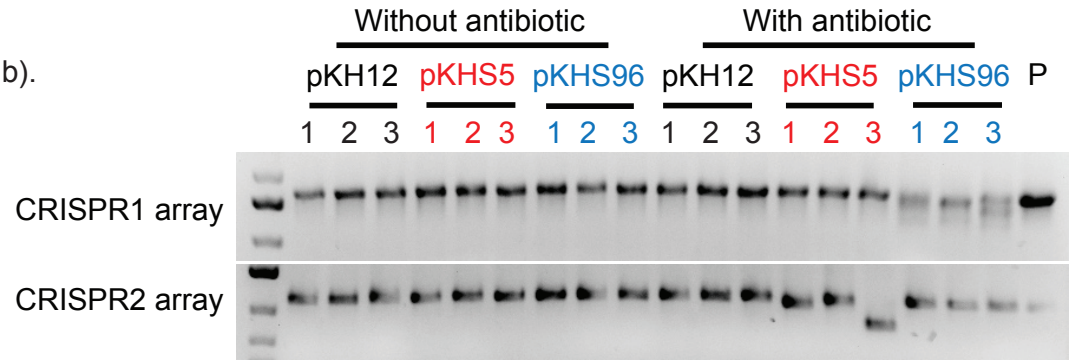

Figure 7. Antibiotic-driven CRISPR compromisation is conserved in all type II CRISPR-Cas systems in *E. faecalis*. a) Plasmid maintenance rates of OG1RF transformants passaged in the absence of chloramphenicol. Each dot represents the average rate from three transformants with the standard deviation. b) CRISPR1 and CRISPR2 amplicon PCR results from Day 14 transformant populations passaged without antibiotic (left) and with antibiotic (right). P: positive control.

813 **Table 1. Bacterial strains and plasmids used.**
814

Name	Description	Reference
***E. faecalis* strains**		
T11RF	Rifampicin- and fusidic acid-resistant derivative of the human urine isolate T11	(32, 53)
T11RFΔ*cas9*	Derivative of T11RF with *cas9* deleted	(32)
T11RFΔ*recA*	Derivative of T11RF with *recA* deleted	This study
OG1RF	Rifampicin- and fusidic acid-resistant derivative of the human oral isolate OG1	(21, 54)
OG1SSp	Spectinomycin- and streptomycin-resistant derivative of OG1; donor strain for conjugation assays	(42, 43, 45)
Plasmids		
pAM714	65 kb PRP encoding erythromycin on Tn*917*, derivative of pAD1	(43)
pCF10	67 kb PRP encoding tetracycline resistance on Tn*925*	(45)
pLZ12	Broad host range shuttle vector encoding chloramphenicol resistance	(55)
pKH12	pLZ12 with *oriT*	(56)
pKHS5	pKH12 with CRISPR2 protospacer S5 and CRISPR1/2 PAM	This study
pKHS96	pKH12 with CRISPR1 protospacer S96 and CRISPR1/2 PAM	(39)
pWH*recA*	pLT06 with ~750 bp up- and downstream of T11RF *recA*	This study
pVP107	pLT06 with T11CR2 protospacer and CRISPR1/2 PAM	(32)
pWH107	pVP107 digested with XbaI/SphI and re-ligated with primers pVP107_ XbaI _For/pVP107_SphI_Rev to remove PstI enzyme site	This study
pWH107.S1	pWH107 with T11CR3 protospacer S1 and CRISPR3 PAM inserted between BamHI/PstI	This study
pWH107.S6	pWH107 with T11CR3 protospacer S6 and CRISPR3 PAM inserted between BamHI/PstI	This study
pWH107.S7	pWH107 with T11CR3 protospacer S10 and CRISPR3 PAM inserted between BamHI/PstI	This study

815

816

817 **Table 2. CRISPR alleles.**
818

Sample name	Day 1 Sanger[c]	Day 14 Sanger[c]	Day 1 Amplicon[d]	Day 14 Amplicon[d]
T11RF control[a]	WT	WT	WT	WT
Δ4[b]	WT	WT	WT	WT
WT1[b]	Poor quality at S_6-S_7	WT	ΔS_6 ΔS_6-S_7	WT
WT2[b]	WT	ΔS_2-S_{11}	WT	ΔS_2-S_{11}
WT3[b]	Poor quality at S_6-S_7	ΔS_5-S_7	ΔS_6 ΔS_5-S_7	ΔS_5-S_7 ΔS_6
WT5[b]	Poor quality at S_3-S_8	Poor quality at S_3-S_9	ΔS_5-S_8 ΔS_3-S_{16} ΔS_6 ΔS_4-S_9 ΔS_1-S_{14}	ΔS_5-S_8 ΔS_4-S_9 ΔS_6 ΔS_6-S_{18} ΔS_3-S_{16}
WT6[b]	Poor quality at S_1-S_7	Poor quality at S_5-S_6	ΔS_5-S_6 ΔS_1-S_{17} ΔS_5-S_7 ΔS_6 ΔS_6-S_9	ΔS_6 ΔS_5-S_6 ΔS_5-S_7 ΔS_6-S_{10}

819 [a]T11RF without pAM714 passaged for 14 days in BHI medium.
820 [b]pAM714 transconjugants passaged for 14 days in BHI medium with erythromycin.
821 [c]CRISPR3 alleles detected by Sanger sequencing.
822 [d]CRISPR3 alleles detected by Illumina amplicon deep sequencing. Mutant alleles with >0.3%
823 abundance are shown for each population and are listed from highest to lowest abundance. If
824 no mutant alleles were detected above this threshold, "WT" is stated.
825

826

827 **Table 3. Nonsynonymous *cas9* mutations detected by whole genome sequencing.**
828

Position	Ref	Allele	Amino acid change	WT1[a]	WT2[a]	WT3[a]
652983	G	A	Gln506*	31.6% (689x)	ND (590x)	ND (577x)
653184	C	T	Glu439Lys	ND (640x)	ND (536x)	24.2% (594x)
653180	AG	T	Leu440fs	ND (640x)	ND (528x)	23.5% (590x)
654165	G	-	Arg112fs	ND (676x)	48.4% (659x)	ND (772x)

829 [a]Shown are variation frequency and coverage at the indicated nucleotide position on *E. faecalis* T11
830 contig 1.11.
831 ND, not detected.

832

833 **Supporting Information Figure Legends**

834 **Figure S1. *E. faecalis* possesses two Type II CRISPR-Cas systems and one orphan**
835 **CRISPR.** a) Schematic mechanism of Type II CRISPR-Cas defense in bacteria. Upon MGE
836 invasion, CRISPR-Cas acts as a genome defense system. When a new MGE is encountered,
837 the protospacer is recognized based on Protospacer Adjacent Motif (PAM). A complex of Cas
838 proteins incorporates the protospacer into the leader end of CRISPR array to form a new spacer
839 (Adaptation). During the expression stage, the CRISPR array is transcribed into pre-crRNA,
840 which is further processed into mature crRNA by Cas9, tracrRNA and a host-encoded
841 endonuclease. The mature crRNA consists of part of a repeat and part of a spacer, which is
842 bound to a Cas9:tracrRNA complex to form an effector complex. When the previously
843 encountered MGE invades again, the effector complex recognizes the target by sequence
844 complementarity and the presence of a PAM. Upon recognition, the target is cleaved and thus
845 invasion by the MGE is blocked. The definition of R, TR and S_n is described in Material and
846 Methods. b). CRISPR-Cas loci occurring in *E. faecalis* T11RF and OG1RF. *E. faecalis* T11RF
847 encodes a CRISPR3-Cas system and a CRISPR2 array. S_6 within the CRISPR3 array targets
848 pAM714 and pWH107.S6, while S_1 and S_7 within CRISPR3 array target pWH107.S1 and
849 pWH107.S7, respectively. *E. faecalis* OG1RF encodes a CRISPR1-Cas system and a

CRISPR2 array. S_4 within CRISPR1 array targets pKHS96, while S_6 within CRISPR2 array targets pKHS5.

Figure S2. Initial phenotypes of select transconjugants. a) Frequency of pAM714 carriage in transconjugant colonies used to initiate serial passage experiments. b) CRISPR3 amplicon PCR results for transconjugant colonies used to initiate serial passage experiments. Shown are CRISPR3 amplicon sizes for six T11RF pAM714 transconjugants (WT 1-6), a representative T11RFΔ*cas9* pAM714 transconjugant (Δ4), T11RF genomic DNA as a positive control (P), and a reagent control (N).

Figure S3. Gel electrophoresis of CRISPR3 amplicons in T11RF pAM714 transconjugants over 14 days passaged with and without antibiotic. Six T11RF pAM714 transconjugants were serially passaged for 14 days in BHI (left panel) or BHI with erythromycin (right panel). The size of the CRISPR3 array was monitored using PCR and gel electrophoresis on each passage day.

Table S1. Primers used in this study.

Table S2. SNPs detection in all gDNA sequencing samples.

Table S3. Quality control of the amplicon sequencing reads.